INSTITUTE OF PHYSICS PUBLISHING JOURNAL OF PHYSICS: CONDENSED MATTER

J. Phys.: Condens. Matter **17** (2005) S3997–S4014 doi:10.1088/0953-8984/17/47/024

Chemical and mechanical efficiencies of molecular motors and implications for motor mechanisms

Hongyun Wang

Department of Applied Mathematics and Statistics, University of California, Santa Cruz, CA 95064, USA

E-mail: hongwang@ams.ucsc.edu

Received 30 August 2005
Published 4 November 2005
Online at stacks.iop.org/JPhysCM/17/S3997

Abstract

Molecular motors operate in an environment dominated by viscous friction and thermal fluctuations. The chemical reaction in a motor may produce an active force at the reaction site to directly move the motor forward. Alternatively a molecular motor may generate a unidirectional motion by rectifying thermal fluctuations using free energy barriers established in the chemical reaction. The reaction cycle has many occupancy states, each having a different effect on the motor motion. The average effect of the chemical reaction on the motor motion can be characterized by the motor potential profile. The biggest advantage of studying the motor potential profile is that it can be reconstructed from the time series of motor positions measured in single-molecule experiments. In this paper, we use the motor potential profile to express the Stokes efficiency as the product of the chemical efficiency and the mechanical efficiency. We show that both the chemical and mechanical efficiencies are bounded by 100% and, thus, are properly defined efficiencies. We discuss implications of high efficiencies for motor mechanisms: a mechanical efficiency close to 100% implies that the motor potential profile is close to a constant slope; a chemical efficiency close to 100% implies that (i) the chemical transitions are not slower than the mechanical motion and (ii) the equilibrium constant of each chemical transition is close to one.

(Some figures in this article are in colour only in the electronic version)

1. Introduction

Protein motors play a central role in many cell functions. For example, myosin drives muscle contraction, kinesin drives intracellular vesicle transportation, and the V-ATPases regulate intracellular acidity. Understanding the operating principles of protein motors is crucial to comprehending intracellular protein transport and cell motility.

Due to the small size of molecular motors, the motor motion is dominated by viscous friction and thermal fluctuations [4]. As a result, molecular motors have several properties that distinguish them from macroscopic motors. For molecular motors,

(1) the effect of inertia is negligible, or more precisely the timescale of inertia is much smaller than the timescale of a reaction cycle;
(2) the instantaneous velocity, caused by thermal fluctuations, is several orders of magnitude larger than the average velocity; and
(3) the kinetic energy of the motor corresponding to the average velocity is a tiny fraction of the free energy consumption per reaction cycle.

In contrast, for macroscopic motors, the timescale of inertia is much larger than the timescale of a reaction cycle; the instantaneous velocity is approximately the same as the average velocity; and the kinetic energy of the motor corresponding to the average velocity is a very large multiple of the free energy consumption per reaction cycle. Therefore, we should not simply extend all results for macroscopic motors to molecular motors without examining them carefully. In both macroscopic motors and molecular motors, a unidirectional motion can be generated by producing an active force at the chemical reaction site and using the active force to drive the motor forward. This mechanism of generating a unidirectional motion is called the power stroke motor mechanism [42, 25]. However, in molecular motors, a unidirectional motion can also be generated by a completely different mechanism. In the one-dimensional motion, if thermal fluctuations in one direction are blocked, then the motor will be carried forward by thermal fluctuations in the other direction. This mechanism of generating a unidirectional motion is called the Brownian ratchet mechanism [29, 12, 23, 2, 32]. The information ratchet discussed in [3] corresponds to the Brownian ratchet in this paper. In a Brownian ratchet, the motor is moved forward by thermal fluctuations and there is no active force produced at the chemical reaction site to drive the motor forward. Of course, the free energy for the unidirectional motion comes from the chemical reaction, which establishes the energy barriers blocking the backward fluctuations. In a Brownian ratchet, the kinetic energy flow from the chemical reaction site to the motor motion is zero. Furthermore, for molecular motors, the kinetic energy flow from the chemical reaction site to the motor motion may be negative or may even exceed the free energy consumption of the motor [43]. Thus, the kinetic energy flow in molecular motors is completely different from that in macroscopic motors. This indicates that we should be especially careful when studying the efficiencies of molecular motors.

When a motor is working against a conservative force, the thermodynamic efficiency is well defined as the energy conversion efficiency, which is the ratio of energy output to energy input:

$$\eta_{\text{Thermodynamics}} = \frac{\text{Energy output per time}}{\text{Energy input per time}}.$$

Here the energy output is the potential energy increase in the external agent exerting the conservative force on the motor. This definition is good for both macroscopic motors and molecular motors. For a macroscopic motor working against the viscous friction, in the definition of efficiency, we can simply replace the energy output by the work done on the surrounding fluid (=the friction force times the displacement). This replacement is justified for a macroscopic motor because in one reaction cycle the velocity fluctuation is small and consequently the friction force is nearly uniform. Thus, a macroscopic motor does not see any significant difference between working against the viscous friction and working against a conservative force of the same magnitude. In [9, 43], the Stokes efficiency for a molecular motor working against the viscous friction was defined and studied. For a molecular motor, the

velocity fluctuation in one reaction cycle is several orders of magnitude larger than the average velocity. There are at least two candidates for the numerator in the efficiency (to replace the energy output in thermodynamic efficiency): (a) the work done on the surrounding fluid and (b) the average friction force times the displacement. Unfortunately, the work done on the surrounding fluid may be negative or may exceed the energy input [43]. The Stokes efficiency is defined as [9, 43]

$$\eta_{\text{Stokes}} = \frac{\text{Average friction} \times \text{displacement per time}}{\text{Energy input per time}}.$$

Notice that the numerator of the Stokes efficiency does not have a thermodynamic meaning. In particular, it is not the heat put into the surrounding fluid via the motor motion. Therefore, we cannot conclude that $\eta_{\text{Stokes}} \leqslant 100\%$ from simple thermodynamic arguments. In [43], we proved rigorously that $\eta_{\text{Stokes}} \leqslant 100\%$ on the basis of the general mathematical framework for modelling molecular motors, which we will describe in the next section.

The current experimental technologies allow us to measure forces and motions of a single protein motor to the precision of piconewtons and nanometres [37, 17, 14]. Time series of motor positions have been measured for various protein motors at various mechanical loads and chemical concentrations [40, 16, 45, 5, 35]. In the past, only the average velocity and randomness parameter of the motor were extracted from the measured time series of motor positions [40, 36]. In [41], we proposed the concept of a motor force profile and used it to represent the overall effect of the chemical reaction on the motor motion. Mathematically, the motor force profile is a periodic function of the motor position. At each motor position, the motor force profile is the average motor force over all chemical states at that position weighted by the steady state probability densities. The integral of the motor force profile is called the motor potential profile, which is a tilted periodic function. The most important property of the motor potential profile is that it can be reconstructed from measured time series of motor positions [41]. Thus, the potential profile is a measurable quantity that provides insight into the motor mechanism. For a Brownian ratchet, the potential profile is a sequence of vertical free energy drops rectifying forward fluctuations while the potential profile of a power stroke motor is a gradually decreasing function of the motor position, generating an active force to drive the motor. Brownian ratchet and power stroke motors are two extreme situations. The potential profile of a motor may have both vertical free energy drops and downhill slopes. There is no guarantee that the motor potential profile will be monotonic. So it may also have vertical barriers and uphill slopes. The motor potential profile is the link between the chemical reaction and the motor motion. We can conceptually divide the motor into two parts: first the chemical reaction produces the potential profile; then the potential profile produces the motor motion. In this paper, we consider the Stokes efficiency and use the motor potential profile to decompose it as the product of the chemical efficiency and mechanical efficiency. The chemical efficiency measures how efficiently the chemical reaction generates the motor potential profile. The mechanical efficiency measures how efficiently the potential profile generates the motor motion. We will show that the chemical efficiency and the mechanical efficiency are both bounded by 100%. Thus, they are both properly defined efficiencies. For the overall Stokes efficiency to be near 100%, both the chemical efficiency and the mechanical efficiency must be near 100%. If the mechanical efficiency is near 100%, then the potential profile must be close to a constant slope downhill. If the chemical efficiency is near 100%, then first the chemical transitions are not rate limiting (i.e., the chemical transitions are not slower than the mechanical motion over the transition region) and second the free energy change associated with each transition is close to zero (i.e., the equilibrium constant of each chemical transition is close to one). In this paper the 'chemical transition' means the 'change of occupancy'. Below, we will first introduce the mathematical formulation for describing molecular motors. Then

we review the Stokes efficiency and the motor potential profile. After that we will decompose the Stokes efficiency into the chemical efficiency and the mechanical efficiency and show that both efficiencies are bounded by 100%. Finally we discuss the implications for the motor mechanism if the chemical efficiency or the mechanical efficiency or both are near 100%.

2. Mathematical formulation of molecular motors

In general, a molecular motor has many degrees of freedom, of which one is associated with the unidirectional motion of the motor. For example, a kinesin dimer walks along a microtubule [39, 15, 40, 8], and the γ shaft of the FoF_1 ATP synthase rotates with respect to the $\alpha_3\beta_3$ hexamer [1, 34, 24, 42, 22]. In studies of molecular motors, it is natural to follow the motor along the dimension of its unidirectional motion [30, 18, 2, 12], and model the other degrees of freedom in the mean field potential affecting the unidirectional motion.

We consider the one-dimensional motion of a small particle in a fluid environment subject to a potential, $V(x)$, where x is the coordinate along the dimension of the unidirectional motion. The particle is subject to the force derived from the potential, the viscous drag force, and the Brownian force. The drag force is the mean of the random force caused by the bombardments of surrounding fluid molecules. The drag force always opposes the motion. The Brownian force is the rest part of the random force. The mean of the Brownian force is zero. The stochastic motion of the particle is governed by the Langevin equation with inertia (Newton 's second law):

$$m\frac{\mathrm{d}v}{\mathrm{d}t} = -\underbrace{\zeta v}_{\substack{\text{Drag}\\ \text{force}}} - \underbrace{V'(x)}_{\substack{\text{Force from}\\ \text{potential}}} + \underbrace{\sqrt{2k_{\mathrm{B}}T\zeta}\,\frac{\mathrm{d}W(t)}{\mathrm{d}t}}_{\substack{\text{Brownian}\\ \text{force}}} \tag{1}$$

where m is the mass and v the velocity of the particle. In the above, $W(t)$ is the Weiner process. The drag force on the particle, ζv, is proportional to the velocity, and ζ is called the drag coefficient. The magnitude of the Brownian force is related to the drag coefficient, and is given by $\sqrt{2k_{\mathrm{B}}T\zeta}$. This is a result of the fluctuation-dissipation theorem [31]. Here k_{B} is the Boltzmann constant and T the absolute temperature [21].

2.1. Reduction to the Langevin equation without inertia

Molecular motors operate in an environment dominated by viscous friction and thermal fluctuations. For molecular motors, equation (1) has two very different timescales: the very short timescale for the motor 'forgetting' about its initial velocity and the relatively long timescale for the motor motion driven by the potential. It is analytically and computationally convenient and necessary to get rid of the short timescale (i.e., ignore the effect of inertia) and approximate equation (1) using the Langevin equation without inertia. To give an intuitive picture of the timescales and the approximation, let us consider a bead of radius r. The drag coefficient and the mass of the bead are, respectively, given by [4]

$$\zeta = 6\pi\eta r, \qquad m = \tfrac{4}{3}\pi\rho r^3$$

where ρ is the density of the bead and η the viscosity of the surrounding fluid. We consider the quantity $t_0 = \frac{m}{\zeta} = \frac{2\rho}{9\eta}\,r^2$. It has the dimension of time and it is proportional to the square of the bead radius. Consequently, for a small bead, the timescale t_0 is very small. For a latex bead of 0.5 μm in water, we have $\rho = 10^{-21}$ g nm^{-3}, $\eta = 0.01$ P $= 10^{-9}$ pN nm^{-2} s, $r = 250$ nm,

and the timescale t_0 is $t_0 = \frac{m}{\zeta} = \frac{2\rho}{9\eta} r^2 \approx 14 \times 10^{-9}$ s $= 14$ ps. This timescale is much smaller than the timescale of motor reaction cycles. We rearrange terms in equation (1) to write it as

$$\frac{\mathrm{d}v}{\mathrm{d}t} = -\frac{1}{t_0}\left(v - \left[-\frac{1}{\zeta}V'(x) + \sqrt{2D}\,\frac{\mathrm{d}W(t)}{\mathrm{d}t}\right]\right) \tag{2}$$

where $D = \frac{k_B T}{\zeta}$ is the diffusion constant [4]. When t_0 is very small the solution of (2) satisfies approximately

$$v = \left[-\frac{1}{\zeta}V'(x) + \sqrt{2D}\,\frac{\mathrm{d}W(t)}{\mathrm{d}t}\right]. \tag{3}$$

The reduction from (2) to (3) in the limit of small t_0 is called the Einstein–Smoluchowski limit [33]. The reduction from (2) to (3) can be illustrated intuitively by considering a simple model differential equation similar to (2):

$$\frac{\mathrm{d}v}{\mathrm{d}t} = -\frac{1}{t_0}(v - f(t)). \tag{4}$$

The solution of (4) is given by

$$v(t) = f(t) + \exp\left(\frac{-t}{t_0}\right)(v(0) - f(t)) + \frac{1}{t_0}\int_0^t \exp\left(\frac{-(t-s)}{t_0}\right)(f(s) - f(t))\,\mathrm{d}s. \tag{5}$$

When t_0 is very small and for $t > 0$, the solution of (4) satisfies approximately $v(t) = f(t)$. A more rigorous analysis of the reduction from (2) to (3) can be found in [33]. We write (3) as a differential equation for x:

$$\frac{\mathrm{d}x}{\mathrm{d}t} = -\frac{1}{\zeta}\,[-f + V'_S(x)] + \sqrt{2D}\,\frac{\mathrm{d}W(t)}{\mathrm{d}t}. \tag{6}$$

Here we have replaced the potential $V(x)$ by an external force f plus a periodic potential $V_S(x)$, which may vary with S, the current chemical occupancy state of the reaction site. This is for the convenience of the discussion below. Equation (6) is the Langevin equation without inertia, governing the stochastic motion of a small particle driven by the external force f and potential $V_S(x)$.

2.2. *Modelling changes of occupancy*

In molecular motors, the motion is not driven by a static potential. Rather, it is driven by switching among a set of potentials, each corresponding to a chemical occupancy state. Thus, in equation (6), the periodic potential $V_S(x)$ changes with the current chemical occupancy state S of the motor system [30, 12]. It is important to point out that in this mathematical framework, the overall chemical process in the motor system is divided into two kinds of chemical steps: those chemical steps that involve changes of occupancy of catalytic sites and those that do not. In this mathematical framework, all chemical steps involving changes of occupancy are modelled as chemical transitions and are governed by a discrete Markov process. Chemical steps that do not involve changes of occupancy are modelled as a continuous conformational change on the potential curve of the corresponding occupancy state. For ATPase motors, the ATP hydrolysis cycle at each catalytic site goes through four occupancy states [1, 6, 44, 7]:

$$\mathrm{Site} + \mathrm{ATP} \overset{\text{Binding}}{\longleftrightarrow} \mathrm{Site}\cdot\mathrm{ATP} \overset{\text{Hydrolysis}}{\longleftrightarrow} \mathrm{Site}\cdot\mathrm{ADP}\cdot\mathrm{P_i}$$
$$\overset{\mathrm{P_i}\ \text{Release}}{\longleftrightarrow} \mathrm{Site}\cdot\mathrm{ADP} + \mathrm{P_i} \overset{\text{ADP Release}}{\longleftrightarrow} \mathrm{Site} + \mathrm{ADP} + \mathrm{P_i}.$$

The whole ATP hydrolysis cycle involves more than just the change of occupancy. For example, 'an ATP diffusing into a catalytic site and being weakly bound' involves a change of occupancy

of the catalytic site and is modelled as a chemical transition (a jump in the discrete Markov process). On the other hand, 'the ATP going from being weakly bound to being tightly bound' does not involve a change of occupancy and is modelled as a sliding down along the potential curve corresponding to the ATP occupancy state.

Suppose the chemical reaction cycle has N occupancy states. The discrete Markov process describing the stochastic evolution of the occupancy state can be symbolically written as

$$\frac{\mathrm{d}S(t)}{\mathrm{d}t} = K(x) \cdot S(t) \tag{7}$$

where $S(t) = \{S_1, S_2, \ldots, S_N\}$ represents the set of all occupancy states of the motor system, and $K(x) = \{k_{Sj}(x)\}$ is the transition matrix. For $j \neq S$, $k_{Sj}(x) = k_{j\to S}(x)$ is the rate of transition from occupancy state j to state S. The diagonal elements of $K(x)$ are defined as $k_{SS}(x) = -\sum_{j\neq S} k_{S\to j}(x)$. Notice that, in molecular motors, the chemical transition is generally coupled to the mechanical motion. As a result, the transition rate $k_{j\to S}(x)$ is a function of the motor position. The stochastic evolution of a motor system (mechanical motion and chemical transition) is governed by Langevin equation (6) coupled with discrete Markov process (7).

In experiments, only average quantities (such as the average velocity and effective diffusion) can be measured reliably. All average quantities can be calculated from the probability density of the motor. Let us consider an ensemble of motors, each evolving in time independently and stochastically according to equations (6) and (7). Let $\rho_S(x,t)$ be the probability density for the motor being at position x and in occupancy state S at time t. The time evolution of $\rho_S(x,t)$ is governed by the Fokker–Planck equation corresponding to (6) and (7) [33, 13]:

$$\frac{\partial \rho_S}{\partial t} = D\frac{\partial}{\partial x}\left(\underbrace{\frac{-f + V_S'(x)}{k_\mathrm{B}T}\rho_S}_{\substack{\text{Effects of external}\\ \text{and motor forces}}} + \underbrace{\frac{\partial \rho_S}{\partial x}}_{\substack{\text{Brownian}\\ \text{motion}}}\right) + \underbrace{\sum_{j=1}^{N} k_{j\to S}(x)\rho_j}_{\text{Chemical reactions}}, \qquad S = 1, 2, \ldots, N. \tag{8}$$

Equation (8) is a general mathematical framework for theoretical discussion of molecular motors [30, 28, 11, 32, 10, 43, 26]. It is important to point out that although (8) is a linear differential equation in terms of the probability density, it is nonlinear in terms of the vector $(\rho_S, V_S, D, k_{j\to S})$. In general, the motor system does not respond linearly to changes in $(V_S, D, k_{j\to S})$. So deciphering the motor mechanism is definitely not a linear problem.

2.3. Detailed balance and reaction diagrams

In modelling molecular motors, the transition rates in (8) cannot be arbitrarily specified. They must satisfy detailed balance. Detailed balance is a condition on transition rates that ensures that, if the system is brought to equilibrium, the probability density is given by the Boltzmann distribution. Detailed balance is an equilibrium property while molecular motors operate in the non-equilibrium mode. We impose detailed balance on the transition rates because, in the mathematical framework described above, the transition rates do not 'know' whether or not the system is in equilibrium. Indeed, the transition rates in equation (8) depend only on the motor position. That is, at a given motor position, the transition rates are not affected if transition rates at other locations are changed (for example, some transitions are blocked) to bring the system to equilibrium. Specifically, detailed balance requires that the rates of transition between two

states A and B satisfy

$$\frac{k_{A\to B}}{k_{B\to A}} = \exp\left(\frac{G_A - G_B}{k_B T}\right) \tag{9}$$

where G_A and G_B are the free energies of, respectively, states A and B. We have to be careful in assigning free energy to a chemical state. To illustrate the subtlety, we consider a simple situation where the motor has only one catalytic site, and, in each cycle, it goes through N chemical states sequentially ($N > 2$):

$$\cdots \leftrightarrow S_N \underbrace{\leftrightarrow S_1 \leftrightarrow S_2 \leftrightarrow \cdots \leftrightarrow S_{N-1} \leftrightarrow S_N}_{\text{One reaction cycle}} \leftrightarrow S_1 \leftrightarrow \cdots \tag{10}$$

We define $V_j(x)$ as the free energy of the motor at position x in chemical state S_j when the motor is in the particular reaction cycle specified in the diagram above. In the diagram, the chemical state S_N immediately to the left of the specified reaction cycle has free energy $V_N(x) + A$ and the chemical state S_1 immediately to the right of the specified reaction cycle has free energy $V_1(x) - A$ where $A = -\Delta G$ is called the chemical affinity [19, 20] and $\Delta G < 0$ is the free energy drop in one reaction cycle. For example, for the ATP hydrolysis cycle at physiological conditions, $-\Delta G \approx 20 k_B T$ [38]. In the simple situation shown in diagram (10), detailed balance requires the transition rates in (8) to satisfy

$$\begin{aligned} &\frac{k_{j\to j+1}(x)}{k_{j+1\to j}(x)} = \exp\left(\frac{V_j(x) - V_{j+1}(x)}{k_B T}\right) \qquad \text{for } 1 \leqslant j < N \\ &\frac{k_{N\to 1}(x)}{k_{1\to N}(x)} = \exp\left(\frac{V_N(x) - V_1(x) + A}{k_B T}\right). \end{aligned} \tag{11}$$

The situation is most confusing when a cycle has only two chemical states as shown below:

$$\cdots \underset{\leftarrow}{\longrightarrow} S_2 \underbrace{\underset{k^-_{1\to 2}}{\overset{k^+_{2\to 1}}{\rightleftarrows}} S_1 \underset{k^-_{2\to 1}}{\overset{k^+_{1\to 2}}{\rightleftarrows}} S_2}_{\text{One reaction cycle}} \underset{k^-_{1\to 2}}{\overset{k^+_{2\to 1}}{\rightleftarrows}} S_1 \underset{\leftarrow}{\longrightarrow} \cdots \tag{12}$$

For reaction diagram (12), the transition rate $k_{1\to 2}(x)$ in the mathematical framework described above, for example, contains both $k^+_{1\to 2}$, the transition from S_1 forward to S_2, and $k^-_{1\to 2}$, the transition from S_1 backward to S_2. For each transition, we can impose detailed balance:

$$\begin{aligned} &k_{1\to 2}(x) = k^+_{1\to 2}(x) + k^-_{1\to 2}(x), \\ &k_{2\to 1}(x) = k^+_{2\to 1}(x) + k^-_{2\to 1}(x), \\ &\frac{k^+_{1\to 2}(x)}{k^-_{2\to 1}(x)} = \exp\left(\frac{V_1(x) - V_2(x)}{k_B T}\right), \\ &\frac{k^-_{1\to 2}(x)}{k^+_{2\to 1}(x)} = \exp\left(\frac{V_1(x) - V_2(x) - A}{k_B T}\right). \end{aligned}$$

Consequently, for the transition rates $k_{1\to 2}(x)$ and $k_{2\to 1}(x)$, we have

$$\frac{k_{1\to 2}(x)}{k_{2\to 1}(x)} \neq \exp\left(\frac{V_1(x) - V_2(x)}{k_B T}\right). \tag{13}$$

Unfortunately (13) is sometimes viewed as the breaking of detailed balance. This view is a direct result of viewing the chemical reaction as a system jumping between two *fixed* states, each state having a *fixed* free energy:

$$S_1 \underset{k_{2\to 1} = k^+_{2\to 1} + k^-_{2\to 1}}{\overset{k_{1\to 2} = k^+_{1\to 2} + k^-_{1\to 2}}{\rightleftarrows}} S_2.$$

In reality, the free energies of S_1 and S_2 depend on the number of reaction cycles that have already been completed. Therefore, we believe, for the discussion of free energy, it is more reasonable to view the chemical reaction as a system going along an infinite sequence of sets of N states as shown in diagrams (10) and (12). This is especially important for avoiding confusion when the reaction cycle has only two states.

3. Thermodynamic efficiency and Stokes efficiency

3.1. Thermodynamic efficiency

In single-molecule experiments, if a motor works against a conservative force from an external agent (such as the force from a laser trap), then the energy input is the chemical free energy consumed by the motor and the energy output is the potential energy increase in the external agent that exerts the conservative force. In this case, the thermodynamic efficiency is well defined as the energy conversion efficiency:

$$\eta_{\text{Thermodynamics}} = \frac{-fv}{Ar} \tag{14}$$

where $A = -\Delta G$ is the chemical affinity, f the external force, v the average velocity, and r the reaction rate (average number of reaction cycles per time). Here the external force is defined as positive if it is in the same direction as the unloaded motor motion. So a load force that opposes the motor motion is negative.

3.2. Stokes efficiency

In many single-molecule experiments it is only possible to load a molecular motor by manipulating the viscous drag from the fluid medium. For example, Yasuda *et al* [45] measured the rotational velocities of the F_1 ATPase motor driving actin filaments of various sizes. In these situations, there is no energy output to increase the potential energy of an external agent, and, as a result, the thermodynamic efficiency does not apply. It is tempting to define an efficiency as the heat generated via the motor motion divided by the chemical energy consumption. However, an efficiency measure must be between zero and one. As we will see later, *the heat generated via the motor motion may be negative or may exceed the free energy consumption*. In [9, 43], the Stokes efficiency was defined to measure how efficiently the motor is utilizing the chemical energy to generate a unidirectional motion in a viscous fluid medium:

$$\eta_{\text{Stokes}} = \frac{\zeta v^2}{Ar + fv} \tag{15}$$

where ζ is the drag coefficient. In [43], we proved rigorously that the Stokes efficiency is between zero and one, and, thus, it is a properly defined efficiency. The proof in [43] was based on the mathematical formulation (8) described in the previous section. In appendix A, we will give another proof, which is independent of equation (8) but is valid only for a motor system in the linear regime where it is not far from equilibrium.

3.3. Two examples

To illustrate the subtlety associated with the discussion of Stokes efficiency, we show two examples. In the first example, the work done on the surrounding fluid via motor motion (the heat generated via the motor motion) is negative. That is, the kinetic energy flows from the fluid environment to the motor motion and then to the catalytic site. In the second example,

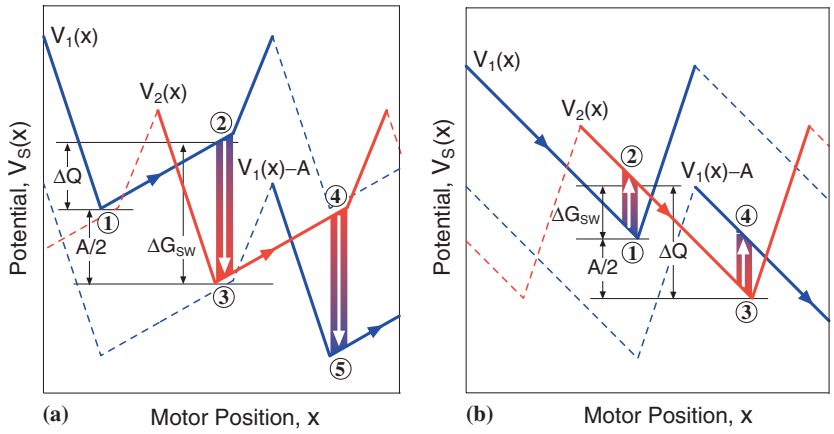

Figure 1. Two hypothetical motor systems. (a) A system in which the work done on the surrounding fluid via motor motion is negative. (b) A system in which the work done on the surrounding fluid via motor motion exceeds the free energy consumption of the motor.

the work done on the surrounding fluid via motor motion exceeds the free energy consumption of the motor.

In figure 1(a), ① → ② → ③ represents one half of one reaction cycle. The second half, ③ → ④ → ⑤, is identical to the first half except that it is shifted in the spatial direction by half of the motor step and shifted in the free energy direction by half of the chemical affinity. The motor system starts at ①. Potential $V_1(x)$ does not directly drive the motor forward. Rather, for the motor to move forward, it has to diffuse uphill along potential $V_1(x)$ from ① to ②. The kinetic energy for the motor to move from ① to ② comes from thermal fluctuations (the heat in the surrounding fluid). In the process of ① to ②, the surrounding fluid does work on the motor motion. In other words, the work done on the surrounding fluid via motor motion is negative. Of course, it is impossible to extract heat repeatedly from the environment to do work for free. The work done by the surrounding fluid on the motor motion and the uphill fluctuation from ① to ② is rectified by the chemical transition from ② to ③. During the chemical transition from ② to ③, the catalytic site of the motor may exchange heat with the surrounding fluid. But no work is done via the motor motion during the chemical transition. In ① → ② → ③, the heat generated via the motor motion is negative. A possible realization of this hypothetical system is the case where positive ions diffuse through a membrane pore against a voltage difference, driven by a concentration gradient. In this case, kinetic energy (heat) is absorbed by ions to diffuse through the membrane pore against the voltage difference. Once on the other side of the membrane, the heat absorption and the diffusion are rectified by the concentration difference.

In figure 1(b), ① → ② → ③ represents one half of one reaction cycle. The motor system starts at ①. For the motor to move forward, it has to make an uphill chemical transition from ① to ② (a change of occupancy that will switch the motor system from potential $V_1(x)$ to potential $V_2(x)$). No work is done via the motor motion during the chemical transition. Once on potential $V_2(x)$, the motor is driven by $V_2(x)$ from ② to ③. In the process of downhill sliding from ② to ③, kinetic energy flows from potential $V_2(x)$ to the motor motion then as heat to the surrounding fluid. In this process, the amount of heat generated via the motor motion is determined by the positions of ② and ③ on potential $V_2(x)$, and is independent of the free energy difference between ① and ②. If we shift $V_1(x)$ vertically relative to $V_2(x)$, it will change ΔG_{SW}, the free energy difference associated with the transition from ① to ②.

But the vertical shifting will not change ΔQ, the amount of heat generated via the motor motion in the sliding from ② to ③. When ΔG_{SW} is negative, as shown in figure 1(b), ΔQ is larger than $A/2$, the free energy consumed in ① → ② → ③. A possible realization of this hypothetical system is the case where positive ions are driven through a membrane pore by a voltage difference against a concentration gradient. In this case, energy flows from the voltage difference to the ion motion then as heat to the environment. Because the ion motion also builds up a concentration gradient, the free energy consumed is less than the heat generated via the ion motion. Another possible realization of figure 1(b) is the F_1 ATPase motor. The power stroke driven by the ATP binding transition from weak binding to strong binding does a fixed amount of work on the surrounding fluid via motor motion [45, 25]. This fixed amount of work is not affected by the ATP concentration in solution. The ATP concentration in solution affects the frequency of the power stroke and the free energy change of the hydrolysis cycle. When the ATP concentration is low, the amount of work done via motor motion exceeds the free energy consumption.

4. Motor potential profile

In single-molecule experiments, time series of motor positions are recorded [40, 45, 46]. However, these time series have not been fully utilized. In the past, only a value of the average velocity and sometimes a value of the randomness parameter were extracted from each time series [40, 36]. These time series actually contain much more information. At least, we can reconstruct the motor potential profile (a function of motor position, defined below) from each time series.

At each position, besides the passive viscous drag on the motor, the motor is subject to two other forces: the motor force corresponding to the current occupancy state, $V_S'(x)$, and the Brownian force from the surrounding fluid, $\sqrt{2k_BT\zeta}\,\frac{dW(t)}{dt}$. The Brownian force is stochastic. The motor force, in general, is also stochastic. This is because even if the motor position is given, the current chemical occupancy state is unknown and its evolution is stochastic. *In theory*, the sum of these two forces and the current chemical state can be observed. Then, at each motor position and in each chemical state, we can average the total force over time to get rid of the Brownian force. So *in theory*, the motor force as a function of position for each chemical occupancy state can be recovered from the full accurate observation of both motor position and chemical occupancy state. However, the current experimental technologies have not yet allowed us to record both the motor position and the chemical occupancy state. It is still an open problem how much information about the motor system we can deduce from the time series of motor positions. For the time being, we believe it is unrealistic to reconstruct all N potential curves corresponding to the N chemical occupancy states. From the time series of motor positions, *in principle*, we can calculate the total force on the motor at each position (this is not the actual method that we are going to use to reconstruct the motor potential profile). The total force is stochastic. At each motor position, we can average the total force over time to get rid of the Brownian force. The result is the average motor force as a function of position, which is periodic and is called the motor force profile. The integral of the motor force profile is a tilted periodic function, and is called the motor potential profile. Here, in averaging over time at each position, implicitly we are averaging over all chemical states weighted by steady state probabilities of these states at each position.

4.1. Mathematical definition of the motor potential profile

Let us define the motor force/potential profile in the mathematical framework (8). We consider the case where the external force is zero: $f = 0$. At the steady state, summing all N component

equations in system (8), we have

$$0 = D\frac{\partial}{\partial x}\left(\frac{\psi'(x)}{k_{\mathrm{B}}T}\rho + \frac{\partial \rho}{\partial x}\right) \tag{16}$$

where $\rho(x) = \sum_{S=1}^{N} \rho_S(x)$ is the steady state probability density for the motor being at position x (regardless of the chemical occupancy state). In (16), all reaction terms cancel with each other because the transition matrix satisfies the property $k_{SS}(x) = -\sum_{j\neq S} k_{S\to j}(x)$. The motor potential profile, $\psi(x)$, is defined as

$$\psi'(x) = \frac{1}{\rho(x)}\sum_{S=1}^{N} V_S'(x)\rho_S(x). \tag{17}$$

In [30], an effective potential for a two-state model was considered in a similar way. Equation (16) shows that the steady state probability density $\rho(x)$ behaves as if the motor were driven by the potential $\psi(x)$. In this sense, the motor potential profile represents the overall effect of the chemical reaction on the motor motion. Because $\psi'(x)$ is periodic with period L (usually the motor step size), we can write $\psi(x)$ as $\psi(x) = \phi(x) - \frac{\Delta\psi}{L}x$ where $\phi(x)$ is a periodic function. $\Delta\psi = \psi(0) - \psi(L) > 0$ can be viewed as the potential energy made available in the chemical reaction per motor step for driving the motor motion.

4.2. Extracting the motor potential profile from data

Equation (17) does not provide us with a direct way of calculating the potential profile $\psi(x)$ from experimental data. Let us look at how the motor potential profile can be reconstructed from the time series of motor positions. In equation (16), the steady state probability flux is

$$J = -D\left(\frac{\psi'(x)}{k_{\mathrm{B}}T}\rho + \frac{\partial \rho}{\partial x}\right). \tag{18}$$

The probability flux is related to the average velocity as $J = \frac{v}{L}$. So J is calculated from average velocity, which can be measured reliably from the time series. In terms of J and $\rho(x)$, we express the motor potential profile as

$$\frac{\psi(x)}{k_{\mathrm{B}}T} = -\log(\rho(x)) - \frac{J}{D}\int_0^x \frac{1}{\rho(s)}\,\mathrm{d}s + C.$$

Thus, to reconstruct $\psi(x)$, we only need to recover $\rho(x)$ from the time series. Mathematically, recovering $\rho(x)$ from the time series can be done in a much more reliable way than by differentiating the time path to calculate the stochastic force. Still it is a numerical challenge to recover $\rho(x)$ reliably, especially when only a limited number of experimental data are available. This numerical issue will be addressed in a separate paper.

5. Chemical and mechanical efficiencies

The motor potential profile $\psi(x)$ serves as a link between the chemical reaction and the motor motion. $\Delta\psi = \psi(0) - \psi(L)$ can be viewed as the potential energy made available in the chemical reaction per motor step for driving the motor motion. $\Delta\psi$ is generated by the chemical reaction and is used to drive the motor motion. We would like to investigate how efficiently $\Delta\psi$ is generated in the chemical reaction and how efficiently $\Delta\psi$ is utilized in driving the motor motion. For that purpose, we write the Stokes efficiency as the product of two terms. Here we consider the case where the external force is zero, $f = 0$:

$$\eta_{\mathrm{Stokes}} = \frac{\zeta v^2}{Ar} = \eta_{\mathrm{Chemical}} \cdot \eta_{\mathrm{Mechanical}} \tag{19}$$

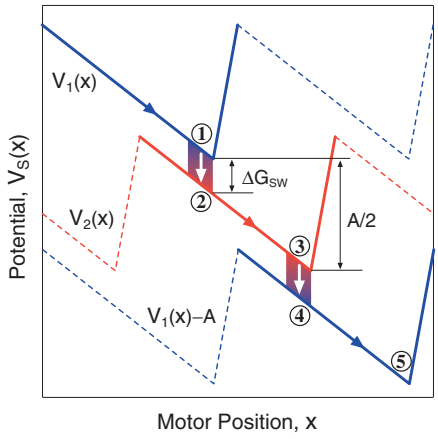

Figure 2. A hypothetical motor system used to study the behaviours of the chemical efficiency and the mechanical efficiency.

where η_{Chemical} and $\eta_{\text{Mechanical}}$ are defined as

$$\eta_{\text{Chemical}} = \left(\frac{\Delta\psi}{Ar\frac{L}{v}}\right), \qquad \eta_{\text{Mechanical}} = \left(\frac{\zeta v L}{\Delta\psi}\right). \tag{20}$$

In the definition of η_{Chemical}, the numerator is $\Delta\psi$ and the denominator is $Ar\frac{L}{v}$, which is the free energy consumed per motor step. η_{Chemical} measures how efficiently $\Delta\psi$ is generated in the chemical reaction per motor step, so we call it the chemical efficiency of the motor. In $\eta_{\text{Mechanical}}$, the denominator is $\Delta\psi$ and the numerator is $\zeta v L$, which is proportional to the average velocity, the mechanical performance of the motor. In this sense, $\eta_{\text{Mechanical}}$ measures how efficiently $\Delta\psi$ is utilized to drive the motor through the viscous media (against viscous friction). So we call it the mechanical efficiency of the motor. However, for these to be properly defined efficiencies, they must be bounded by 100%. In appendix B, we show that both the chemical efficiency and the mechanical efficiency defined above are indeed bounded by 100%.

Now we study the behaviour of these two efficiencies in a hypothetical motor system. In particular, we investigate what factors are responsible for reducing the overall Stokes efficiency from 100%. We consider the system shown in figure 2.

In figure 2, a motor is driven by switching along an infinite sequence of sets of two potentials. ① → ② → ③ represents one half of a reaction cycle. In ① → ② → ③, the displacement is $\frac{L}{2}$ and the free energy consumption is $\frac{A}{2}$. The two potentials are selected as

$$V_1(x) = E\begin{cases}\dfrac{-8x}{7L} & \text{for } 0 \leqslant x \leqslant \frac{7L}{8} \\ \dfrac{-8(L-x)}{L} & \text{for } \frac{7L}{8} \leqslant x \leqslant L,\end{cases} \qquad V_1(x+L) = V_1(x)$$

$$V_2(x) = V_1\left(x - \frac{L}{2}\right) - \frac{A}{2}.$$

We use the parameters $E = 30k_{\text{B}}T$, $L = 16$ nm, and $D = 4000$ nm^2 s^{-1}. Here we study a tightly coupled motor in which the transition between $V_1(x)$ and $V_2(x)$ is restricted to the region $[\frac{6L}{8}, \frac{7L}{8}]$. The activation energy barrier for the transition ① to ② is $\Delta G_{\text{SW}} = \frac{4}{7}E - \frac{A}{2}$. In

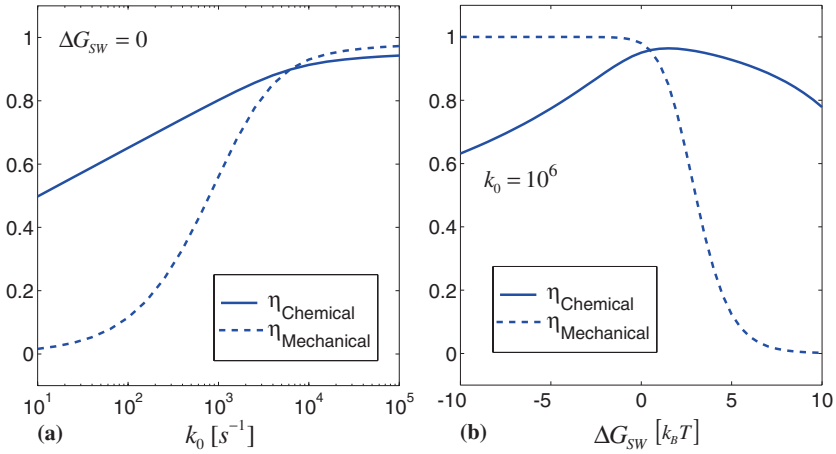

Figure 3. The chemical efficiency and the mechanical efficiency (a) as functions of the transition rate and (b) as functions of the activation energy barrier of the transition.

simulations below, the chemical affinity A is determined by setting the energy barrier $\Delta G_{\rm SW}$. We use the transition rates

$$k_{1\to 2} = k_0 \exp\left(\frac{-\Delta G_{\rm SW}}{k_{\rm B}T}\right), \qquad k_{2\to 1} = k_0$$

which satisfies detailed balance (11). We first set $\Delta G_{\rm SW} = 0$ and study the effect of k_0 on the chemical and mechanical efficiencies.

Case 1: $\Delta G_{SW} = 0$ and k_0 is varied

Figure 3(a) shows the two efficiencies as functions of k_0. It is clear that as k_0 is decreased, both efficiencies are reduced, especially the mechanical efficiency. This is not surprising. Since the reaction and the motion are tightly coupled, a motor step depends on the completion of a reaction cycle. When the reaction rate is decreased, the motor waits a long time at ① for the transition ① to ② to occur. As a result, the average velocity is reduced. The long waiting time at ① makes the probability accumulate near ①, which leads to a bump near ① in the motor potential profile. As we analyse in appendix B, when a motor potential profile deviates from a constant slope, the mechanical efficiency is reduced. The accumulation of the probability near ① also brings the negative slope region into the average in the motor potential profile. Consequently $\Delta\psi$ is reduced and so is the chemical efficiency. Therefore, slow reaction rates reduce both the chemical component and the mechanical component of the Stokes efficiency.

Now we fix k_0 at a large value and study the effect of $\Delta G_{\rm SW}$ on the two efficiencies.

Case 2: $k_0 = 10^6$ and ΔG_{SW} is varied

Figure 3(b) shows the two efficiencies as functions of $\Delta G_{\rm SW}$. When $\Delta G_{\rm SW}$ is negative, the transition ① to ② is energetically favourable; at the end of each motor step, the system quickly jumps to the next potential and starts the next motor step; and the delay between steps is minimal. As a result, the average velocity is optimal, no probability is accumulated near ①, and the motor potential profile is close to having a constant slope. So the mechanical efficiency is close to 100%. However, a negative $\Delta G_{\rm SW}$ also increases the free energy consumed per motor step, but it does not increase $\Delta\psi$. This can be seen from the definition of $\psi(x)$. The

derivative of $\psi(x)$ is an average of the derivatives of $V_1(x)$ and $V_2(x)$, which does not increase if the free energy drop from ① to ② is made bigger and bigger. Consequently, when ΔG_{SW} is negative and its magnitude is increased, the chemical efficiency is reduced. When ΔG_{SW} is positive, the transition ① to ② is energetically unfavourable; at the end of each motor step, the system waits a long time near ① for the transition ① to ② to occur before the next motor step can start; and the delay between steps increases as the free energy barrier ΔG_{SW} increases. So, the average velocity is significantly reduced, the probability is accumulated near ①, and the motor potential profile deviates from a constant slope. As a result, the mechanical efficiency is reduced significantly when ΔG_{SW} is positive and is increased. The accumulation of probability near ① also brings the negative slopes of $V_1(x)$ and $V_2(x)$ into the average in the motor potential profile, which will reduce $\Delta\psi$. Thus, unfavourable reaction steps will reduce the chemical efficiency. This decrease in the chemical efficiency is less prominent because the unfavourable reaction steps, in general, will also reduce the free energy consumption, the denominator in the chemical efficiency.

In summary, the Stokes efficiency is reduced in both the positive region and the negative region of the transition free energy difference ΔG_{SW}. Therefore, the optimal situation is achieved if the equilibrium constant associated with each occupancy change is about one.

6. Conclusions

Molecular motors convert chemical energy to generate unidirectional motion against conservative force and/or viscous friction while operating in an isothermal environment dominated by viscous friction and thermal fluctuations. Because of the small size, molecular motors have several properties that distinguish them from macroscopic motors. For molecular motors,

(i) the effect of inertia is negligible, or more precisely the timescale of inertia is much smaller than the timescale of a reaction cycle;
(ii) the instantaneous velocity, caused by thermal fluctuations, is several orders of magnitude larger than the average velocity; and
(iii) the kinetic energy of the motor corresponding to the average velocity is a small fraction of the free energy consumption per reaction cycle.

For example, for a kinesin dimer pulling a bead of 1 μm with an average velocity of 1000 $\mu\mathrm{m\ s}^{-1}$, the kinetic energy of the bead corresponding to the average velocity is less than $1.3 \times 10^{-7} k_{\mathrm{B}}T$. The free energy consumed in each hydrolysis cycle of the kinesin dimer is about $20 k_{\mathrm{B}}T$. The chemical reaction in a molecular motor may produce an active force at the reaction site to directly move the motor forward (a power stroke motor). Alternatively a molecular motor may generate a unidirectional motion by rectifying thermal fluctuations using the free energy barriers produced in the chemical reaction (a Brownian ratchet). The chemical reaction cycle has many occupancy states. For example, the ATP hydrolysis cycle at a catalytic site has four occupancy states. In general, each occupancy state may have a different effect on the motor motion. Since the current experimental technologies have not yet allowed us to record both motor position and chemical occupancy state, it is not realistic to recover details about the effect of each individual occupancy state on the motor motion. We use the motor potential profile to characterize the average effect of the chemical reaction on the motor motion. The most important feature of the motor potential profile is that it can be reconstructed from the time series of motor positions measured in single-molecule experiments. Here the small size of molecular motors plays a very interesting role. On one hand, the effort of deciphering the motor mechanism is, in many respects, hindered by the small size. On the

other hand, the small size eliminates the effect of inertia and makes it possible to uncover the motor force profile from time series. In contrast, for macroscopic motors, the effect of inertia lasts over many reaction cycles. As a result, it is virtually impossible to determine the force profile of a macroscopic motor from recorded motor positions. In this paper, we use the motor potential profile to decompose the Stokes efficiency as the product of the chemical efficiency and the mechanical efficiency. Under the mathematical framework for modelling molecular motors, we show that both the chemical and mechanical efficiencies are bounded by 100%, and, thus, are properly defined efficiencies. Using a hypothetical motor system, we investigate the behaviour of these two efficiencies for different reaction rates and for different activation free energy barriers of chemical transitions. The mechanical efficiency is completely determined by the shape of the motor potential profile. If the mechanical efficiency is close to 100%, then the motor potential profile must be close to a constant slope. The chemical efficiency depends on the reaction kinetics. If the chemical efficiency is close to 100%, then it places two conditions on the motor system: (i) the chemical transitions are not rate limiting and (ii) the free energy change associated with each chemical transition is close to zero. Condition (i) concerns both the chemical reaction and the mechanical motion and can be achieved by slowing down the mechanical motion. Condition (ii) concerns only the chemical reaction. Condition (ii) implies that in an optimal situation, the equilibrium constant associated with each change of occupancy should be close to one. In the F_1 ATPase, the equilibrium constant associated with the hydrolysis (ATP $\leftrightarrow$ ADP Pi) inside the catalytic site is, indeed, close to one [6].

Acknowledgment

This work was partially supported by NSF Grant DMS-0317937.

Appendix A. Stokes efficiency for a system near equilibrium

In this appendix, we show that for a motor system in the linear regime where it is not far from equilibrium, $\eta_{\text{Stokes}} \leqslant 1$ can be argued to be independent of mathematical formulation (8). It is important to point out that this argument is valid only for systems near equilibrium. We use an approach similar to that used in [27].

The average velocity and reaction rate are functions of the external force, f, and the chemical affinity, $A = -\Delta G$:

$$v = v(f, A), \qquad r = r(f, A).$$

In the absence of chemical free energy and the external force, the system is at equilibrium:

$$v(0, 0) = r(0, 0) = 0.$$

When the system is close to equilibrium, we can expand v and r to linear terms:

$$v(f, A) = \lambda_{11} f + \lambda_{12} A, \qquad r(f, A) = \lambda_{21} f + \lambda_{22} A. \tag{21}$$

In the linear regime, the Onsager relation holds [19]: $\lambda_{21} = \lambda_{12}$. Substituting into (14) and using the fact that the thermodynamic efficiency is always bounded by 1, we have

$$\lambda_{11} f^2 + 2\lambda_{12} f A + \lambda_{22} A^2 \geqslant 0 \qquad \text{for all values of } f \text{ and } A,$$

which leads to $\lambda_{12}^2 \leqslant \lambda_{11}\lambda_{22}$. In the absence of chemical free energy ($A = 0$), (21) relates the velocity to the external force as $v = \lambda_{11} f$. Thus, we identify $\zeta = 1/\lambda_{11}$. Substituting into the Stokes efficiency (15), we obtain

$$\eta_{\text{Stokes}} = \frac{\zeta v^2}{Ar + fv} = \frac{\lambda_{11} f^2 + 2\lambda_{12} f A + (\lambda_{12}^2/\lambda_{11}) A^2}{\lambda_{11} f^2 + 2\lambda_{12} f A + \lambda_{22} A^2} \leqslant 1.$$

Therefore, in the linear regime, the Stokes efficiency is bounded by 100%.

Appendix B. Chemical and mechanical efficiencies are bounded by 100%

In this appendix, we show that the chemical efficiency and the mechanical efficiency defined in (20) are bounded by 100%.

We first show that the chemical efficiency is bounded by 100%. For that purpose, we need to show that $\Delta\psi\frac{v}{L} \leqslant Ar$. We rewrite the steady state of equation (8) in the conservative form

$$0 = -J_S' + I_{S-1\to S} - I_{S\to S+1}, \qquad S = 1, 2, \ldots, N \tag{22}$$

where

$$\begin{aligned} J_S &= -D\left(\frac{V_S'}{k_BT}\rho_S + \rho_S'\right) = -D\rho_S F_S', \qquad F_S = \frac{V_S}{k_BT} + \log(\rho_S) \\ I_{S\to S+1} &= \rho_S k_{S\to S+1} - \rho_{S+1}k_{S+1\to S}. \end{aligned} \tag{23}$$

Here J_S is the probability flux in the motion direction for chemical state S and $I_{S\to S+1}$ is the probability flux density in the reaction direction from state S to state $S+1$. The transition rates $k_{S\to S+1}$ and $k_{S+1\to S}$ satisfy detailed balance (11). From the definition of $\psi(x)$ in (17), we have

$$\Delta\psi = \psi(0) - \psi(L) = -\int_0^L \frac{1}{\rho}\sum_{S=1}^N V_S'\rho_S\,\mathrm{d}x. \tag{24}$$

Using the relation $V_S'\rho_S = -\frac{k_BT}{D}(J_S + D\rho_S')$ derived from (23), we get

$$\Delta\psi = \frac{k_BT}{D}\int_0^L \frac{1}{\rho}\sum_{S=1}^N (J_S + D\rho_S')\,\mathrm{d}x = \frac{k_BT}{D}\int_0^L \frac{1}{\rho}\sum_{S=1}^N J_S\,\mathrm{d}x. \tag{25}$$

The average velocity is related to the probability fluxes as $\frac{v}{L} = \sum_{S=1}^N J_S$. In particular, the sum of probability fluxes over all states is independent of x. Multiplying (25) by $\frac{v}{L}$, using (23) to give $J_S = -\sqrt{\rho_S}\cdot\sqrt{\rho_S}DF_S'$, and applying the Cauchy–Schwarz inequality in the summation, we obtain

$$\begin{aligned} \Delta\psi\frac{v}{L} &= \frac{k_BT}{D}\int_0^L \frac{1}{\rho}\left[\sum_{S=1}^N J_S\right]^2\mathrm{d}x = \frac{k_BT}{D}\int_0^L \frac{1}{\rho}\left[\sum_{S=1}^N -\sqrt{\rho_S}\cdot\sqrt{\rho_S}DF_S'\right]^2\mathrm{d}x \\ &\leqslant \frac{k_BT}{D}\int_0^L \frac{1}{\rho}\left[\sum_{S=1}^N \rho_S\right]\left[\sum_{S=1}^N \rho_S D^2\left(F_S'\right)^2\right]\mathrm{d}x = -k_BT\int_0^L\sum_{S=1}^N J_S F_S'\,\mathrm{d}x. \end{aligned} \tag{26}$$

Integrating by parts and using (22) yields

$$\Delta\psi\frac{v}{L} \leqslant k_BT\int_0^L\sum_{S=1}^N F_S\left(I_{S-1\to S} - I_{S\to S+1}\right)\mathrm{d}x. \tag{27}$$

Because the chemical reaction is periodic, we have

$$I_{0\to 1} = I_{N\to N+1}, \qquad V_{N+1} = V_1 - A, \qquad F_{N+1} = F_1 - \frac{A}{k_BT}. \tag{28}$$

Applying summation by parts in (27) and using the periodic condition (28), we arrive at

$$\Delta\psi\frac{v}{L} \leqslant k_BT\int_0^L\sum_{S=1}^N I_{S\to S+1}\left(F_{S+1} - F_S\right)\mathrm{d}x + A\int_0^L I_{N\to N+1}\,\mathrm{d}\theta. \tag{29}$$

In (29), the integrand in the first integral on the right-hand side has the form

$$I_{S\to S+1}\left(F_{S+1} - F_S\right) = \rho_S k_{S\to S+1}(1-H)\log(H), \qquad H = \frac{\rho_{S+1}}{\rho_S}\exp\left(\frac{V_{S+1} - V_S}{k_BT}\right).$$

Function $(1-H)\log(H)$ is always non-positive for any value of H. The second integral in (29) is the chemical reaction rate r. Thus, (29) leads immediately to $\Delta\psi\frac{v}{L} \leqslant Ar$.

Now we show that the mechanical efficiency is bounded by 100%. For that purpose, we need to show that $\frac{\zeta v L}{\Delta\psi} \leqslant 1$. In (16), the steady state probability density satisfies

$$\rho'(x) + \frac{\psi'(x)}{k_B T}\rho(x) = \frac{-v}{LD}.$$

Multiplying by the integration factor and integrating from s to $s+L$, we get

$$\exp\left(\frac{\psi(s)-\Delta\psi}{k_B T}\right)\rho(s) - \exp\left(\frac{\psi(s)}{k_B T}\right)\rho(s) = -\frac{v}{LD}\int_0^L \exp\left(\frac{\psi(s+x)}{k_B T}\right)\mathrm{d}x.$$

Dividing by $\exp(\frac{\psi(s)}{k_B T})$ and integrating with respect to s from 0 to L yields

$$\left[1-\exp\left(\frac{-\Delta\psi}{k_B T}\right)\right] = \frac{v}{LD}\int_0^L\int_0^L \exp\left(\frac{\psi(s+x)-\psi(s)}{k_B T}\right)\mathrm{d}x\,\mathrm{d}s.$$

Using $\psi(x) = \phi(x) - \Delta\psi\frac{x}{L}$ and using the change of variables $\hat{x} = \frac{x}{L}$ and $\hat{s} = \frac{s}{L}$, we have

$$\begin{aligned}\frac{\zeta v L}{\Delta\psi} &= \frac{\int_0^1 \exp\left(\frac{-\Delta\psi}{k_B T}\hat{x}\right)\mathrm{d}\hat{x}}{\int_0^1 \exp\left(\frac{-\Delta\psi}{k_B T}\hat{x}\right)h(\hat{x})\,\mathrm{d}\hat{x}},\\ h(\hat{x}) &= \int_0^1 \exp\left(\frac{\phi(\hat{s}L+\hat{x}L)-\phi(\hat{s}L)}{k_B T}\right)\mathrm{d}\hat{s}.\end{aligned} \tag{30}$$

Because $\exp(y)$ is a convex function, applying Jensen's inequality to $h(\hat{x})$, we obtain

$$h(\hat{x}) \geqslant \exp\left(\int_0^1 \frac{\phi(\hat{s}L+\hat{x}L)-\phi(\hat{s}L)}{k_B T}\,\mathrm{d}\hat{s}\right) = 1$$

which, when combined with (30), leads immediately to $\frac{\zeta v L}{\Delta\psi} \leqslant 1$.

If $\phi(x) = 0$ (i.e., $\psi(x)$ is a constant slope), then we have $h(\hat{x}) = 1$ and the mechanical efficiency satisfies $\eta_{\text{Mechanical}} = \frac{\zeta v L}{\Delta\psi} = 1$. Conversely, if the mechanical efficiency is close to 100%, then the motor potential profile $\psi(x)$ must be close to a constant slope measured in units of $k_B T$.

References

[1] Abrahams J, Leslie A, Lutter R and Walker J 1994 Structure at 2.8 Å resolution of F_1-ATPase from bovine heart mitochondria *Nature* **370** 621–8

[2] Astumian R 1997 Thermodynamics and kinetics of a Brownian motor *Science* **276** 917–22

[3] Astumian R D and Derenyi I 1998 Fluctuation driven transport and models of molecular motors and pumps *Eur. Biophys. J.* **27** 474–89

[4] Berg H C 1993 *Random Walks in Biology* (Princeton, NJ: Princeton University Press)

[5] Block S M, Asbury C L, Shaevitz J W and Lang M J 2003 Probing the kinesin reaction cycle with a 2D optical force clamp *Proc. Natl Acad. Sci. USA* **100** 2351–6

[6] Boyer P 1993 The binding change mechanism for ATP synthase—some probabilities and possibilities *Biochim. Biophys. Acta* **1140** 215–50

[7] Boyer P 1997 The ATP synthase—a splendid molecular machine *Annu. Rev. Biochem.* **66** 717–49

[8] Coppin C, Pierce D, Hsu L and Vale R 1997 The load dependence of Kinesin's mechanical cycle *Proc. Natl Acad. Sci. USA* **94** 8539–44

[9] Derenyi I, Bier M and Astumian D 1999 Generalized efficiency and its application to microscopic engines *Phys. Rev. Lett.* **83** 903–6

[10] Dimroth P, Wang H, Grabe M and Oster G 1999 Energy transduction in the sodium F-ATPase of propionigenium modestum *Proc. Natl Acad. Sci. USA* **96** 4924–9

[11] Doering C, Horsthemke W and Riordan J 1994 Nonequilibrium fluctuation-induced transport *Phys. Rev. Lett.* **72** 2984–7
[12] Elston T, Wang H and Oster G 1998 Energy transduction in ATP synthase *Nature* **391** 510–4
[13] Gardiner C 1985 *Handbook of Stochastic Methods* 2nd edn (New York: Springer)
[14] Hirono-Hara Y, Ishizuka K, Kinosita K, Yoshida M and Noji H 2005 Activation of pausing F1 motor by external force *Proc. Natl Acad. Sci. USA* **120** 4288–93
[15] Howard J, Hudspeth A J and Vale R D 1989 Movement of microtubules by single kinesin molecules *Nature* **342** 154–8
[16] Hunt A J, Gittes F and Howard J 1994 The force exerted by a single kinesin molecule against a viscous load *Biophys. J.* **67** 766–81
[17] Itoh H, Takahashi A, Adachi K, Noji H, Yasuda R, Yoshida M and Kinosita K 2004 Mechanically driven ATP synthesis by F1-ATPase *Nature* **427** 465–8
[18] Julicher F, Ajdari A and Prost J 1997 Modeling molecular motors *Rev. Mod. Phys.* **69** 1269–81
[19] Katchalsky A and Curran P 1965 *Nonequilibrium Thermodynamics in Biophysics* (Cambridge, MA: Harvard University Press)
[20] Kondepudi D K and Prigogine I 1998 *Modern Thermodynamics* (New York: Wiley)
[21] Landau L D, Lifshitz E M and Pitaevskii L P 1980 *Statistical Physics* 3rd revised edn (Oxford: Pergamon)
[22] Menz R I, Walker J E and Leslie A G 2001 Structure of bovine mitochondrial F1-ATPase with nucleotide bound to all three catalytic sites: implications for the mechanism of rotary catalysis *Cell* **106** 331–41
[23] Mogilner A and Oster G 1999 The polymerization ratchet model explains the force–velocity relation for growing microtubules *Eur. J. Biophys.* **28** 235–42
[24] Noji H, Yasuda R, Yoshida M and Kinosita K 1997 Direct observation of the rotation of F1-ATPase *Nature* **386** 299–302
[25] Oster G and Wang H 2000 Reverse engineering a protein: the mechanochemistry of ATP synthase *Biochim. Biophys. Acta (Bioenergetics)* **1458** 482–510
[26] Oster G and Wang H 2003 Rotary protein motors *Trends Cell Biol.* **13** 114–21
[27] Parmeggiani A, Julicher F, Ajdari A and Prost J 1999 Energy transduction of isothermal ratchets: generic aspects and specific examples close to and far from equilibrium *Phys. Rev.* E **60** 2127–40
[28] Peskin C S, Ermentrout G B and Oster G F 1994 *Mechanochemical Coupling in ATPase Motors* (*Les Houches*) (Berlin: Springer)
[29] Peskin C S, Odell G M and Oster G 1993 Cellular motions and thermal fluctuations: the Brownian ratchet *Biophys. J.* **65** 316–24
[30] Prost J, Chauwin J, Peliti L and Ajdari A 1994 Asymmetric pumping of particles *Phys. Rev. Lett.* **72** 2652–5
[31] Reif F 1965 *Fundamentals of Statistical and Thermal Physics* (New York: McGraw-Hill)
[32] Reimann P 2002 Brownian motors: noisy transport far from equilibrium *Phys. Rep.* **361** 57–265
[33] Risken H 1989 *The Fokker–Planck Equation* 2nd edn (New York: Springer)
[34] Sabbert D, Engelbrecht S and Junge W 1996 Intersubunit rotation in active F-ATPase *Nature* **381** 623–5
[35] Sambongi Y, Iko Y, Tanabe M, Omote H, Iwamoto-Kihara A, Ueda I, Yanagida T, Wada Y and Futai M 1999 Mechanical rotation of the c subunit oligomer in ATP synthase (F_0F_1): direct observation *Science* **286** 1722–4
[36] Samuel A and Berg H 1995 Fluctuation analysis of rotational speed of the bacterial flagellar motor *Proc. Natl Acad. Sci.* **92** 3502–6
[37] Schnitzer M J and Block S M 1997 Kinesin hydrolyses one ATP per 8-nm step *Nature* **388** 386–90
[38] Stryer L 1995 *Biochemistry* 4th edn (New York: Freeman)
[39] Vale R 1986 Kinesin: possible biological roles for a new microtubule motor *Trends Biochem. Sci.* **11** 464–8
[40] Visscher K, Schnitzer M and Block S 1999 Single kinesin molecules studied with a molecular force clamp *Nature* **400** 184–9
[41] Wang H 2003 Mathematical theory of molecular motors and a new approach for uncovering motor mechanism *IEE Proc. Nanobiotechnol.* **150** 127–33
[42] Wang H and Oster G 1998 Energy transduction in the F1 motor of ATP synthase *Nature* **396** 279–82
[43] Wang H and Oster G 2002 The Stokes efficiency for molecular motors and its applications *Europhys. Lett.* **57** 134–40
[44] Weber J and Senior A E 1997 Catalytic mechanism of F1-ATPase *Biochim. Biophys. Acta* **1319** 19–58
[45] Yasuda R, Noji H, Kinosita K and Yoshida M 1998 F1-ATPase is a highly efficient molecular motor that rotates with discrete 120° steps *Cell* **93** 1117–24
[46] Yasuda R, Noji H, Yoshida M, Kinosita K and Itoh H 2001 Resolution of distinct rotational substeps by submillisecond kinetic analysis of F1-ATPase *Nature* **410** 898–904